BIOCHEMISTRY

 Volume 45, Number 18 May 9, 2006

Articles

Secretory Phospholipase A_2 from *Arabidopsis thaliana*: Insights into the Three-Dimensional Structure and the Amino Acids Involved in Catalysis

Johanna Mansfeld,* Sabine Gebauer, Kristin Dathe,‡ and Renate Ulbrich-Hofmann

Institutes of Biotechnology and Biochemistry, Department of Biochemistry/Biotechnology, Martin-Luther University Halle-Wittenberg, D-06120 Halle, Germany

Received December 16, 2005; Revised Manuscript Received March 7, 2006

ABSTRACT: A low-molecular weight phospholipase A_2 from *Arabidopsis thaliana*, isoform phospholipase A_2-α, has been expressed in *Escherichia coli* in the form of inclusion bodies, refolded, and purified to homogeneity to yield the active mature enzyme. The enzyme was characterized with respect to pH, temperature optimum, and Ca^{2+} ion requirement. The enzyme has been shown to be a true secretory phospholipase A_2 that requires Ca^{2+} ions in the millimolar range and belongs to group XIB. On the basis of the three-dimensional structures of secretory phospholipase A_2 forms ($sPLA_2$s) from bee venom and bovine pancreas, a homology model was generated. Analysis of this model and alignments of different plant $sPLA_2$s showed that the common His-Asp dyad of animal $sPLA_2$s does not exist in plant $sPLA_2$s. In place of the aspartate residue of the dyad, the plant enzymes of group XIA contain a histidine residue, and the enzymes of group XIB contain a serine or an asparagine residue. Mutagenesis of amino acids supposed to be involved in catalysis has shown that His62, the calcium-coordinating Asp63, and the above-mentioned Ser79 residue are essential for activity.

The large phospholipase A_2 (PLA_2)[1] superfamily is defined by the ability of their members to catalyze the hydrolysis of the 2-acyl ester bond of 1,2-diacyl-*sn*-3-phosphoglycerides. According to the localization and the properties of its members, the PLA_2 superfamily is divided into 14 groups (*1*, *2*). On the basis of their structure and function, four different types of PLA_2s can be defined: (i) secretory PLA_2s ($sPLA_2$s) (groups I−III, V, and IX−XIV), (ii) calcium-dependent cytosolic PLA_2s ($cPLA_2$s) (group IV), (iii) calcium-independent cytosolic PLA_2s ($iPLA_2$s) (group VI), and (iv) platelet-activating factor acetyl hydrolases (PAF-AH) (groups VII and VIII).

$sPLA_2$s (EC 3.1.1.4) which hydrolyze phospholipids in a calcium-dependent manner are mainly found in the venoms of snakes and insects, pancreatic juices, and extracellular fluids. Important common structural features are their high disulfide bond content, two well-conserved central helices, high stability, a catalytic His-Asp dyad, a hydrogen bonding network connecting the interfacial binding site and the catalytic site, and a calcium-binding loop. These structural

* To whom correspondence should be addressed: Department of Biochemistry/Biotechnology, Martin-Luther University, Kurt-Mothes-Strasse 3, D-06120 Halle, Germany. Phone: +49 345 5524865. Fax: +49 345 5527303. E-mail: mansfeld@biochemtech.uni-halle.de.

‡Present address: pes Diagnosesysteme, pes Gesellschaft für medizinische Diagnosesysteme mbH, Hauptstrasse 103, D-04416 Leipzig-Markkleeberg, Germany.

[1] Abbreviations: $AtsPLA_2$, secretory phospholipase A_2 from *A. thaliana*; Bis-tris-propane, 1,3-bis[tris(hydroxymethyl)methylamino]-propane; $bpPLA_2$, bovine pancreatic PLA_2; $bvPLA_2$, bee venom PLA_2; Caps, 3-(cyclohexylamino)-1-propanesulfonic acid; DOPC, 1,2-dioleoyl-*sn*-glycero-3-phosphocholine; GdnHCl, guanidine hydrochloride; GSH, reduced glutathione; GSSG, oxidized glutathione; IPTG, isopropyl β-D-thiogalactopyranoside; PC, phosphatidylcholine; PLA_2, phospholipase A_2; PMSF, phenylmethanesulfonyl fluoride; $ppPLA_2$, porcine pancreatic PLA_2; $sPLA_2$, secretory phospholipase A_2; $svPLA_2$, secretory phospholipase A_2 from the venom of *Naja naja*.

10.1021/bi052563z CCC: $33.50
Published on Web 04/13/2006

features have been investigated in detail for many $sPLA_2$s from animal sources and were correlated with the functional properties of these $sPLA_2$s (*3*).

$cPLA_2$s are characterized by a C2 domain at the N-terminus, involved in calcium-mediated phospholipid binding, and the GXSGS motif, which is, like the similar GXSXG consensus motif of lipases, essential for catalysis. The catalytically active serine residue in this motif forms, together with a conserved aspartate residue, the Ser-Asp dyad, which is located in a deep cleft at the center of a predominantly hydrophobic channel (*4*). $iPLA_2$s are also characterized by an active site serine in a lipase consensus motif (*5*).

In comparison to that of animal PLA_2s, the knowledge of PLA_2s from plants is rather poor (*6*). However, within the past decade, some plant cDNAs encoding PLA_2s have been cloned. The corresponding enzymes can be assigned to two different groups. The members of the first group are small secretory PLA_2s (*7*−*14*), which show a significant degree of similarity with animal $sPLA_2$s in the active site and the calcium-binding loop regions. These enzymes belong to groups XIA and XIB (*1*) and will be in the focus of this paper.

The second class of phospholipid-degrading enzymes in plants consists of the patatins. They display nonspecific lipid acyl hydrolase as well as acyl transferase activities and are considered to be storage proteins. Most patatins are localized in the vacuoles (*15*−*17*). Recently, the active sites of cytosolic or partially membrane-bound patatins have been shown to contain a catalytically active Ser-Asp dyad (*18*, *19*). Four members of this class of enzymes are homologous to animal $iPLA_2$s (*20*).

In this paper, we report on the production of one of the four isoforms of $sPLA_2$ from *Arabidopsis thaliana* (AtsPLA$_2$-α) by heterologous expression in *Escherichia coli* and renaturation from inclusion bodies as well as its biochemical characterization. Three-dimensional homology models, generated on the basis of the crystal structures of $sPLA_2$s from bee venom ($bvPLA_2$) and bovine pancreas ($bpPLA_2$), allow first insights into the three-dimensional structures of AtsPLA$_2$-α and -γ. Amino acids supposed to be involved in the catalytic mechanism of AtsPLA$_2$-α are probed by site-directed mutagenesis yielding distinct indications that the catalytic machinery might deviate from that of animal $sPLA_2$s.

MATERIALS AND METHODS

Cloning of AtsPLA$_2$-α. The mature sequence of AtsPLA$_2$-α was amplified by PCR using the *Arabidopsis* EST clone U17374 (TAIR, Arabidopsis Biological Ressource Center, DNA Stock Center, Columbus, OH) as a template and the primers 5′-GGAATTCCATATGCTTAACGTCGGTGTTC-3′ (NdeI) and 5′-CCCAAGCTTACGGTTTCTTGAGGAC-3′ (HindIII) for cloning into pET-26b(+) (MERCK Biosciences, Schwalbach, Germany) (restriction sites for cloning into the vector are underlined). The PCR products were digested with NdeI and HindIII (New England Biolabs, Frankfurt, Germany) and ligated into the vector, which was cut by the same enzymes. The correctness of the nucleotide sequence of the inserts was verified by DNA sequencing using the SequiTherm EXCEL DNA sequencing kit (Epicentre, Madison, WI).

Construction of AtsPLA$_2$-α Variants. The variants H62Q, D63N, S79A, and S79D were created with the QuikChange site-directed mutagenesis kit (Stratagene, La Jolla, CA) according to the instructions of the supplier using wild-type DNA as a template and the following primers: H62Q, 5′-TGTTGCATGAAACA**A**GA**C**GCTTGTGTCCAATC-3′ (forward); D63N, 5′-GTTGCATGAAACAT**A**A**C**GC**G**TGT-GTCCAATCCAAG-3′ (MluI) (forward); S79A, 5′-CTA-AGCCAAGAGTGT**GCA**CAGAAGTTCATTAAC-3′ (ApaLI) (forward); and S79D, 5′-CTAAGCCAAGAGTGT**GA**T-CAGAAGTTCATTAAC-3′ (BclI) (forward) (sites of mutation are marked by bold letters, recognition sequences of introduced restriction sites are underlined, and restriction endonucleases used for screening are given in parentheses). The successful introduction of the mutation was checked by control digestion with the corresponding restriction endonucleases and subsequent DNA sequencing of positive mutant clones. The enzyme variants were produced and purified as described for the wild-type enzyme.

Expression and Isolation of the Protein. Wild-type and mutant proteins were produced in BL21(DE3) cells (MERCK Biosciences, Schwalbach, Germany). Cells were grown in LB medium, supplemented with 25 μg/mL kanamycin, at 37 °C. Expression was induced by addition of 1 mM isopropyl β-D-thiogalactopyranoside (IPTG). Four hours after induction, cells were harvested and disrupted using a Gaulin homogenizer (APV Gaulin, Lübeck, Germany). Inclusion bodies were collected by centrifugation for 15 min at 30000*g* and 4 °C and subsequently solubilized in 100 mM Tris-HCl buffer (pH 8.3) containing 6 M GdnHCl (guanidine hydrochloride), 100 mM DTT, and 1 mM EDTA. After dialysis against 4 M GdnHCl and 20 mM acetic acid, the protein was renatured in 1 M Tris-HCl buffer (pH 8.3−8.5) containing 0.6 mM reduced glutathione (GSH), 3 mM oxidized glutathione (GSSG), 1 mM EDTA, and 11 mM $CaCl_2$ at a protein concentration of 50−75 μg/mL. The renaturation mixture was concentrated by ultrafiltration using a 3 kDa Omega membrane (PALL Filtron, Dreieich, Germany). After buffer exchange on a HiPrep 26/10 desalting column (Pharmacia Biotech, Freiburg, Germany), the enzyme was purified on a MonoQ HR5.5 column (Pharmacia Biotech) equilibrated with 50 mM Tris-HCl buffer (pH 8.5). The protein was eluted with a linear NaCl gradient (from 0 to 0.5 M) in 50 mM Tris-HCl buffer (pH 8.5) and 10 mM $CaCl_2$.

Protein Concentration Determination. Protein concentrations were determined by the Bradford (Sigma, Taufkirchen, Germany) or BCA protein assay (Pierce, Bonn, Germany) with bovine serum albumin as a standard according to the instructions of the supplier.

CD Spectroscopy. CD spectra in the far-UV region were recorded at 20 °C using a Jasco-810 CD spectrophotometer (Labor-und Datentechnik GmbH) in a quartz cell with a path length of 1 mm at a protein concentration of 0.2 mg/mL.

Activity Measurements. PLA_2 activities were routinely determined with 1,2-dioleoyl-*sn*-glycero-3-phosphocholine (DOPC) (kindly donated by Lipoid GmbH, Ludwigshafen, Germany) as the substrate. DOPC (10 mg, 12.7 μmol), dissolved in 200 μL of chloroform and 100 μL of methanol, was dried in a vacuum. The lipid film was dissolved in 600 μL of buffer containing 0.5 M Tris-HCl (pH 8.3), 42 mM Triton X-100, 8 mM SDS, and 42 mM $CaCl_2$ by vortexing

for 15 min. The enzymes were incubated for 5−30 min at 37 °C with 1.3 μmol of substrate in a total volume of 100 μL. Aliquots (10 μL) were removed after defined times of incubation, and the reaction was stopped by addition of 10 μL of 0.2 M EDTA. Initial rates were determined from the increase in the amount of released fatty acid determined by the NEFA C kit (WAKO Chemicals, Neuss, Germany) according to the method of Hoffmann et al. (*21*). The same procedure was used for lysophosphatidylcholine or -ethanolamine from soybean, each of which was also kindly donated by Lipoid GmbH (Ludwigshafen, Germany).

In addition, the $sPLA_2$ kit (Cayman Chemical, Ann Arbor, MI) was used by following the manufacturer's instructions. This kit is based on the detection of free thiols that are formed upon hydrolysis of the thioester bond of 1,2-bis-(heptanoylthio)-PC by $sPLA_2$ using 5,5′-dithiobis(2-nitrobenzoic acid).

Activity toward 1-hexadecanoyl-2-(1-pyrenedecanoyl)-*sn*-glycero-3-phosphocholine was measured according to the method of Radvanyi et al. (*22*).

The influence of phenylmethanesulfonyl fluoride (PMSF) (Sigma, Taufkirchen, Germany) on activity of $AtsPLA_2$-α and porcine pancreatic $sPLA_2$ ($ppPLA_2$) was determined by preincubation of the enzyme solution in the presence of 1 and 2 mM PMSF for 5 min at room temperature and a subsequent activity assay as described above. $ppPLA_2$ (Novo, Bagsvaerd, Denmark) was a gift of Lipoid GmbH and purified by K. Kölbel (Institute of Biotechnology, Halle, Germany) by cation-exchange chromatography (Mono S HR5.5, Pharmacia Biotech).

The influence of *p*-bromophenacylbromide was determined by incubation of the enzyme in the presence of 2 mM *p*-bromophenacylbromide at room temperature.

Determination of the pH Optimum. The following buffers at a concentration of 75 mM were used: acetate buffer (pH 4.5−5.5), Mes buffer (pH 5.5−6.5), Bis-tris-propane buffer (pH 6.5−9.5), Tris-HCl buffer (pH 7.0−8.5), and Caps buffer (pH 9.5−11). The enzyme was incubated with the substrate in the above-mentioned buffers at 37 °C as described above.

Determination of the Temperature Optimum. The enzyme was assayed between 20 and 90 °C at pH 8.3 for 6 min as described above.

Molecular Modeling of $AtsPLA_2$-α and -γ. Homology models of $AtsPLA_2$-α and -γ were built using the homology module COMPOSER of the SYBYL molecular modeling package (SYBYL version 6.9, Tripos Associates Inc., St. Louis, MO) on a Silicon Graphics Octane2 R12000 workstation. BLAST searches provided the related crystal structures of animal $sPLA_2$s [PDB entry 1A3D with a resolution of 1.8 Å (*23*), PDB entry 1POC with a resolution of 2.0 Å (*24*), PDB entry 1P2P with a resolution of 2.6 Å (*25*), and PDB entry 1BP2 with a resolution of 1.7 Å (*26*) (http://us.expasy.org/cgi-bin/blast and http://www.ncbi.nlm.nih.gov/BLAST with identity scores between 30 and 49% and *E*-values between 0.017 and 0.12)] which were used as template structures for homology modeling. The manually created alignment between the selected animal and plant $sPLA_2$s is presented in Figure 1 of the Supporting Information. The models were created as described in detail in the Supporting Information.

To exclude side chain−backbone and side chain−side chain clashes, SCWRL (version 3.0) was applied (*27*). To assess the validity of the homology models, the structures were energy-minimized in a stepwise manner allowing side chain atoms to relax at first followed by backbone atoms before the complete structure was permitted to relax. The Tripos force field, implemented in the SYBYL molecular modeling package, was used for all energy calculations using a distance-dependent dielectric constant of 4, with a non-bonded cutoff of 8 Å. Energy minimization was effected using the Powell algorithm until an energy convergence criterion of 0.05 kcal mol^{-1} $Å^{-1}$ was reached. The stereochemical quality of the models was evaluated using PROCHECK (*28*). The quality of the final models was also checked with PROSA II to examine whether the modeled protein structures contain partially misfolded sequences or represent a natively folded structure (*29*).

RESULTS AND DISCUSSION

Identification and Sequence Analysis of $AtsPLA_2$-α. A BLAST search in the *Arabidopsis* genome sequence database with the sequence of $sPLA_2$ from *Dianthus caryophyllus* (GenBank accession number AF064732) (*9*) as the template showed the existence of four $sPLA_2$ isoenzymes in this plant. The isoenzyme with the highest degree of identity (73%) was present in clone U17374 (GenBank accession number AY136317) (TAIR, Arabidopsis Biological Research Center, Columbus, OH), being identical to the gene of the more recent database entry AY344842 (*14*). The corresponding isoenzyme was named $sPLA_2$-α (*10*). The genes of $AtsPLA_2$-α and -β (GenBank accession number AF541915) are located on chromosome II, loci At2g06925 and At2g19690, whereas the genes of $AtsPLA_2$-γ and -δ (GenBank accession numbers AY148346 and AY148347) are located on chromosome IV, loci At4g29460 and At4g29470.

Clone U17374 consists of 520 bp and contains an open reading frame of 447 bp encoding a protein of 148 amino acids. Using SignalP version 1.1 (http://www.cbs.dtu.dk), a 20-amino acid signal peptide was found.

Sequence alignments of this protein with the presently known plant $sPLA_2$s revealed that $AtsPLA_2$-α can be assigned to group XIB (*1*, *2*) due to its relatively high degree of identity to rice PLA_2 isoform II (GenBank accessionn number AJ238117) (49%). The enzymes from *D. caryophyllus*, isoform II of *Nicotiana tabacum* (GenBank accession number AB190178), the enzymes from *Lycopersicum esculentum* (GenBank accession number SGN-U224692), *Mirabilis jalapa* (GenBank accession number AF064732), and *Gossypium arboreum* (GenBank accession number BF275891), the isoenzymes (GenBank accession numbers BG045671, AW318251, and BE802011) from *Glycine max*, and the enzyme from *Populus tremulus* (GenBank accession number AI164389) with levels of sequence identity with respect to $AtsPLA_2$-α of 72, 61, 59, 48, 39, 39, 37, 39, and 38%, respectively, as well as the enzyme from elm seedlings (*7*) belong to the same group. The enzymes from *N. tabacum*, isoform II, and *L. esculentum* are almost identical to each other (86%).

Isoenzyme I from *Oryza sativa* (GenBank accession number AJ238116), isoenzymes $AtsPLA_2$-β, -γ, and -δ from *A. thaliana*, isoenzyme I from *N. tabacum* (GenBank accession number AB190177), and one of the isoenzymes from *G. max* (GenBank accession number AI522932) can be sorted into group XIA (*1*, *2*). Within this group, the

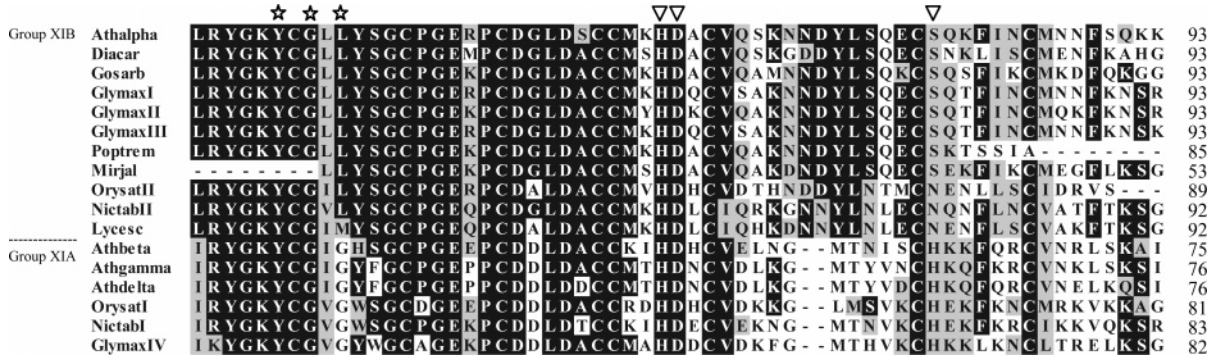

FIGURE 1: Alignment of parts of the amino acid sequences of several $sPLA_2$ from plants. Accession numbers: $sPLA_2$s from *A. thaliana* (AY136317 for Athalpha, AF541915 for Athbeta, AY148346 for Athgamma, and AY148347 for Athdelta), AF064732 for *D. caryophyllus* (Diacar), BF275891 for *Go. arboreum* (Gosarb), BG045671 (GlymaxI), AW318251 (GlymaxII), BE802011 (GlymaxIII), and AI522932 (GlymaxIV) for *G. max*, SGN-U224692 for *L. esculentum* (Lycesc), AY319966 for *M. jalapa* (Mirjal), AB190177 (NictabI) and AB190178 (NictabII) for *N. tabacum*, AJ238116 for *O. sativa* isoform I (Orysat I), AJ238117 for *O. sativa* isoform II (OrysatII), and AI164389 for *Po. tremulus* (Poptrem). Stars denote the amino acid residues involved in calcium binding; triangles denote the amino acid residues putatively involved in catalysis.

isoenzymes $AtsPLA_2$-γ and -δ are almost identical (76%). The comparison of the levels of amino acid identity between $sPLA_2$s from group XIA and XIB yields values between 22 and 32%. All calculations of identities are based on the sequences of the mature proteins. Figure 1 shows the most important part of the alignment of a selection of plant $sPLA_2$s. The whole alignment is available as Figure 2 in the Supporting Information.

Cloning, Recombinant Production, and Purification of $AtsPLA_2$-α. As mentioned by Mansfeld et al. (*12*), the mature sequence of $AtsPLA_2$-α was amplified by PCR and cloned into the NdeI and HindIII sites of pET-26b(+). The $AtsPLA_2$-α gene was expressed in *E. coli* strain BL21(DE3) under standard growth conditions (LB medium, 37 °C, induction with 1 mM IPTG at an OD_{600} of ≈1). The enzyme accumulated in inclusion bodies, which could be isolated in high purity. Expression was also performed in 8 L scale using a fed-batch fermentation process (results not shown).

After solubilization of the protein aggregates with 6 M GdnHCl and partial removal of the denaturant, the enzyme was renatured by reoxidation of the disulfide bonds using the redox shuffling system (GSH/GSSG). The renaturation yield was critically dependent on the composition of the redox shuffling system. Optimal refolding was obtained by fast dilution of the enzyme solution into the refolding buffer to a final protein concentration of 50−75 μg/mL. The concentration of the enzyme solution by ultrafiltration proved to be the critical step due to the strong tendency of the protein to form aggregates, probably caused by the high proportion of hydrophobic amino acids (36%). Homogeneous $AtsPLA_2$-α was finally obtained by anion-exchange chromatography. However, yields of purification processes were still rather low (≤3.5 mg of active protein/L of culture), requiring further optimization.

Experiments to express $AtsPLA_2$-α in *Pichia pastoris* yielded a soluble enzyme but in insufficient yield (results not shown).

Biochemical Characterization of $AtsPLA_2$-α. The purified protein still contained the start methionine as confirmed by N-terminal sequencing and mass spectrometry. The mass of the start Met-containing mature protein was determined to be 14 299.6 Da (calculated molecular mass of 14 299.9 Da).

As proven by CD spectroscopy in the far-UV region (Figure 2), the protein has acquired a native conformation after renaturation. In addition, the activities and biochemical properties of the renatured enzyme were shown to be identical to those of an enzyme obtained in soluble form by expression in *P. pastoris* (results not shown).

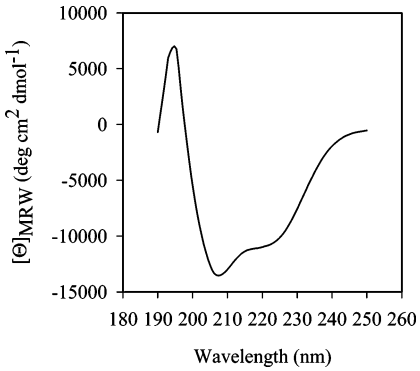

FIGURE 2: Far-UV CD spectra. Spectra were recorded in 50 mM Tris-HCl buffer (pH 8.5) containing 10 mM $CaCl_2$ at a protein concentration of 0.2 mg/mL.

No free fatty acids were liberated when $AtsPLA_2$-α was incubated with lysophosphatidylcholine or -ethanolamine from soybean. With 1-hexadecanoyl-2-(1-pyrenedecanoyl)-*sn*-glycero-3-phosphocholine as the substrate, a labeled fatty acid was detected upon incubation with $AtsPLA_2$-α, classifying $AtsPLA_2$-α clearly as PLA_2.

The specific activity of $AtsPLA_2$-α toward DOPC at 37 °C was 16.7 μmol min^{-1} mg^{-1}. Substrates with short acyl chains and a thioester bond like 1,2-bis(heptanoylthio)-PC were very poor substrates (results not shown). The rather low activities of the plant enzymes might be one of the reasons why these enzymes have been successfully isolated from plant materials only recently (*7*). The temperature optimum of $AtsPLA_2$-α, determined at pH 8.3 with DOPC as the substrate, is between 30 and 40 °C. The enzyme retained 47% of its activity after incubation at 80 °C for 30 min. The enzyme has no activity at 37 °C at pH <6.5. The pH optimum is between pH 8.0 and 9.5. The isoelectric point has been calculated with ProtParam (http://ca.expasy.org/tools/protparam.html) to be 8.0. The experimentally determined isoelectric point is 7.59. The enzyme requires millimolar amounts of $CaCl_2$ and is only marginally active in the absence of calcium ions.

Probably because of its large portion of hydrophobic amino acids, AtsPLA$_2$-α exhibits a strong propensity to aggregate, which unfortunately has prevented attempts to elucidate the tertiary structure by NMR or X-ray crystallography hitherto.

Homology Modeling. Despite the low level of overall sequence identity between the plant enzymes and the enzymes from animal sources (7% for AtsPLA$_2$-α vs bvPLA$_2$, 14% for AtsPLA$_2$-α vs bpPLA$_2$), the regions of the active site and the calcium-binding loop are highly conserved (levels of identity between 31 and 64% in the calcium-binding loop and between 56 and 63% in the region containing the catalytic His residue and the adjacent Ca^{2+}-coordinating Asp residue). Furthermore, 12 cysteine residues are conserved in all plant PLA$_2$s that presumably form six disulfide bonds. This prompted us to generate homology models for AtsPLA$_2$-α and -γ.

The homology models of AtsPLA$_2$-α and -γ are based on the crystal structures of several animal sPLA$_2$s deposited in the Protein Data Bank, especially sPLA$_2$s from the venoms of *Naja Naja* (PDB entry 1A3D) and *Apis mellifera* (PDB entry 1POC) as well as from the pancreas of *Sus scrofa* (PDB entry 1P2P) and *Bos taurus* (PDB entry 1BP2). For AtsPLA$_2$-α, the structure could be modeled between amino acid residues Tyr35 and Cys102 (Figure 3A,B). The analysis of energy-optimized structures regarding its stereochemical quality using PROCHECK (*28*) showed that dihedral angles of all residues were located in most favored (45 residues, 78.9%) and additionally allowed regions (12 residues, 21.1%) of the Ramachandran plot. All other criteria, such as peptide bond planarity and hydrogen bond energy, were within values statistically expected for proteins with a resolution below 2 Å. Additionally, the evaluation of the quality of the modeled structure with PROSA II (*29*) yielded an energy graph below zero and a *z*-score of −4 for the combined energy terms (pair interactions and surface energy terms), which corresponds to scores expected for a native fold of a sequence length of 68 amino acids. This supports the assumption that the modeled protein represents a natively folded structure. The model is also consistent with secondary structure predictions (e.g., PredictProtein at http://www.embl-heidelberg.de/predictprotein). The structures of the N- and C-terminal regions could not be derived because of the very low levels of homology of AtsPLA$_2$-α and -γ to the animal enzymes.

The central part of the molecule of AtsPLA$_2$-α is composed of two antiparallel α-helices formed by amino acid residues Gly54−Asp63 and Gln76−Asn88. This structure is stabilized by two disulfide bonds (Cys58−Cys85 and Cys65−Cys78). The second most important structure element is the highly conserved calcium-binding loop, which is attached to the α-helix with the catalytic His62 residue and the Ca^{2+}-coordinating Asp63 residue by the disulfide bond between Cys39 and Cys59 (Figure 3A). A fourth disulfide bond, which is present in neither bp- nor bvPLA$_2$, can be predicted to exist between Cys46 and Cys102. The other two potential disulfide bonds could not be assigned because three of the cysteines are part of the unmodeled N-terminal region. Besides these structural elements, the structure is characterized by loop structures and two short β-sheets between the α-helices, mainly formed by Lys69, Asn70, Tyr73, and Leu74.

Figure 3B shows that despite large deviations on the primary structure level the tertiary structure of sPLA$_2$s is very well conserved in the regions that are essential for function. The superimposed structures of the calcium-binding loops and the two antiparallel α-helices are nearly identical. The connecting structure elements, however, show a great degree of variability. The shortest one is found in AtsPLA$_2$-α, whereas the two enzymes from animal sources are characterized by large loops and extended β-sheets.

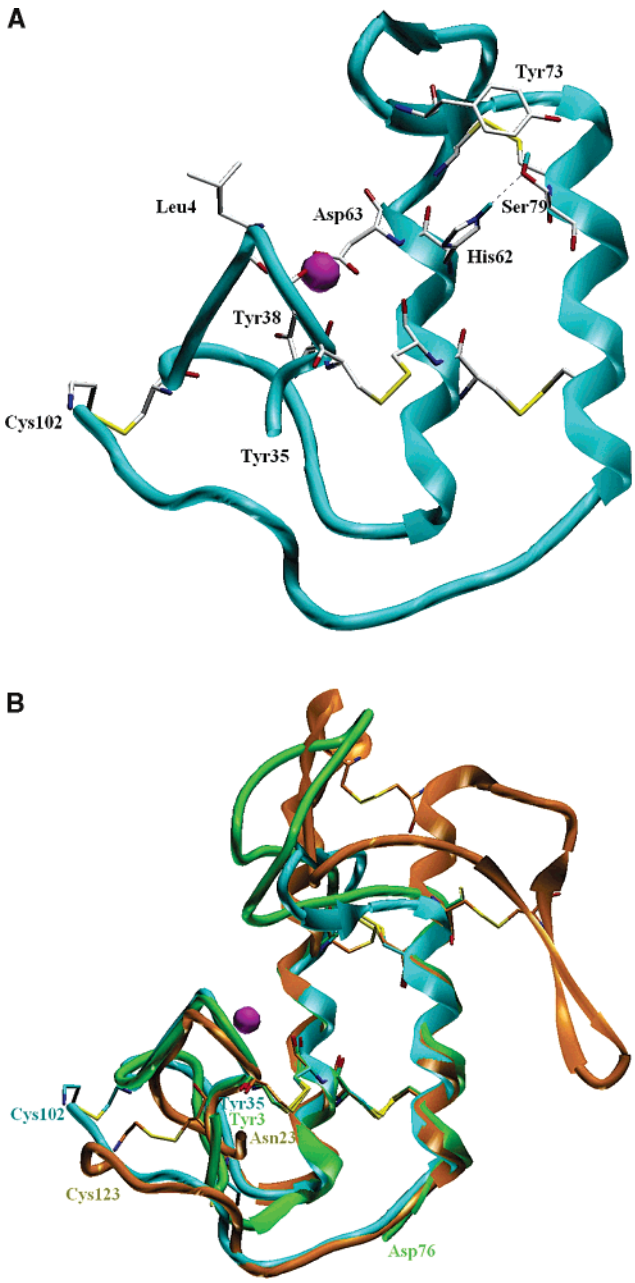

FIGURE 3: Homology model of AtsPLA$_2$-α based on the structures of sPLA$_2$s from bee venom and bovine pancreas. (A) Modeled structure of AtsPLA$_2$-α with the calcium ion (magenta) and the four modeled disulfide bonds (Cys39−Cys59, Cys58−Cys85, Cys65−Cys78, and Cys46−Cys102). (B) Modeled structure of AtsPLA$_2$-α (blue) superimposed with the corresponding regions of the crystal structures of bvPLA$_2$ (green) and bpPLA$_2$ (orange).

Probing the Role of Active Site Residues in the Catalysis by AtsPLA$_2$-α. In literature, two alternative catalytic mechanisms are discussed for sPLA$_2$s. The mechanisms differ by the mode of activation of the water molecule that adopts the role of the serine in serine proteases as the attacking nucleophile. In the mechanism according to Verheij et al.

(*30*), developed for pancreatic sPLA$_2$s, the water molecule is activated by formation of a hydrogen bond to δN of His48 which itself is hydrogen bonded to Asp99 via ϵN. Both amino acids form the catalytic dyad. In the Ca-coordinated oxyanion mechanism (*31*), the catalytic water molecule is coordinated to the calcium ion, and a second water molecule interacts with His48 via δN. In both cases, the calcium ion polarizes the *sn*-2 ester carbonyl group of the substrate. The alcoholate formed during decomposition of the tetrahedral intermediate is protonated by δN of His48.

Modest changes in activity following significant changes in key catalytic residues and in the architecture of the active site, as reported for the D99N mutant of bpPLA$_2$ (*32*), the corresponding D64N mutant of bvPLA$_2$ (*33*), and a H48Q mutant of human sPLA$_2$ (*34*), have shown that there might be a considerable degree of plasticity in the active site. On the other hand, subtle differences in the active site geometry resulted in a less favorable hydrogen bonding network making flow of electrons and transfer of protons more difficult, resulting in less efficient catalysis (*35*, *36*).

Alignment studies as well as the homology model of AtsPLA$_2$-α (Figure 3A) reveal that some of the residues that are highly conserved in animal sPLA$_2$s are not present in the plant enzymes. Especially, the Asp residue of the His-Asp dyad, which is one of the key elements of the catalytic machinery of sPLA$_2$s, does not occur in the plant enzymes. To probe the role of different amino acids in the active site, four variants have been created, and the mutant enzymes have been expressed in *E. coli*. As shown by SDS−PAGE, expression levels and yields of refolded enzyme of all variants were similar to those of the wild-type (results not shown).

Role of His62. The importance of the absolutely conserved catalytic histidine residue [His62 in AtsPLA$_2$-α (Figures 3A and 4A), His34 in bvPLA$_2$ (Figure 4C), and His48 in bp- and ppPLA$_2$] was proven for AtsPLA$_2$-α by construction of the enzyme variant H62Q which had a residual activity of 0.0056% with DOPC as the substrate. This result was also confirmed by inactivation of the enzyme by *p*-bromophenacylbromide, and it is consistent with studies on bp- and ppPLA$_2$ where His48 was replaced with Gln without the loss of conformational stability, but with a drastic loss of activity (residual activity of 0.00014 and 0.0016% for bp- and ppPLA$_2$, respectively) (*35*, *36*).

Role of Asp63. The role of the highly conserved Asp63 of AtsPLA$_2$-α (Figures 3A and 4A), which is like Asp35 of bvPLA$_2$ (Figure 4C) and Asp49 of bp- and ppPLA$_2$ involved in the coordination of the calcium ion and should therefore play an important role in catalysis, was probed by substituting Asp63 with Asn. As shown previously, the analogous D49N mutant of bpPLA$_2$ retained its conformational stability but completely lost its calcium binding capability, and accordingly, the activity was significantly decreased (residual activity of 0.18%) (*37*). Similarly, the D63N mutant of AtsPLA$_2$-α possessed a residual activity of 0.013% toward DOPC, showing the importance of this residue in catalysis for the plant enzyme, too.

Role of Ser79. The three-dimensional model of AtsPLA$_2$-α shows that the position of the aspartate residue (Asp64 of bvPLA$_2$ in Figure 4C and Asp99 in bpPLA$_2$) of the catalytic dyad of animal sPLA$_2$s is occupied by a serine residue (Ser79 in Figures 3A and 4A). To test whether Ser79 plays a role in catalysis, the influence of PMSF, a potent inhibitor of serine proteases (*38*), on activity was determined. As the reaction with PMSF caused a significant activity loss (residual activity of 31.3%) compared to its reaction with ppPLA$_2$ (residual activity of 94.8%), Ser79 of AtsPLA$_2$-α was replaced with Ala or Asp. While the exchange of Ser79 with Ala probes the influence of the hydroxyl group on catalysis with similar spatial requirements, Asp represents the amino acid occurring in animal sPLA$_2$s at this position. Both mutations resulted in a considerable activity loss (residual activity of 0.51 and 0.1% for S79A and S79D, respectively). Therefore, the Ser residue seems to be essential in this position for AtsPLA$_2$-α.

As the alignment with other known plant sPLA$_2$s (Figure 1) shows, this serine residue is conserved in the enzymes

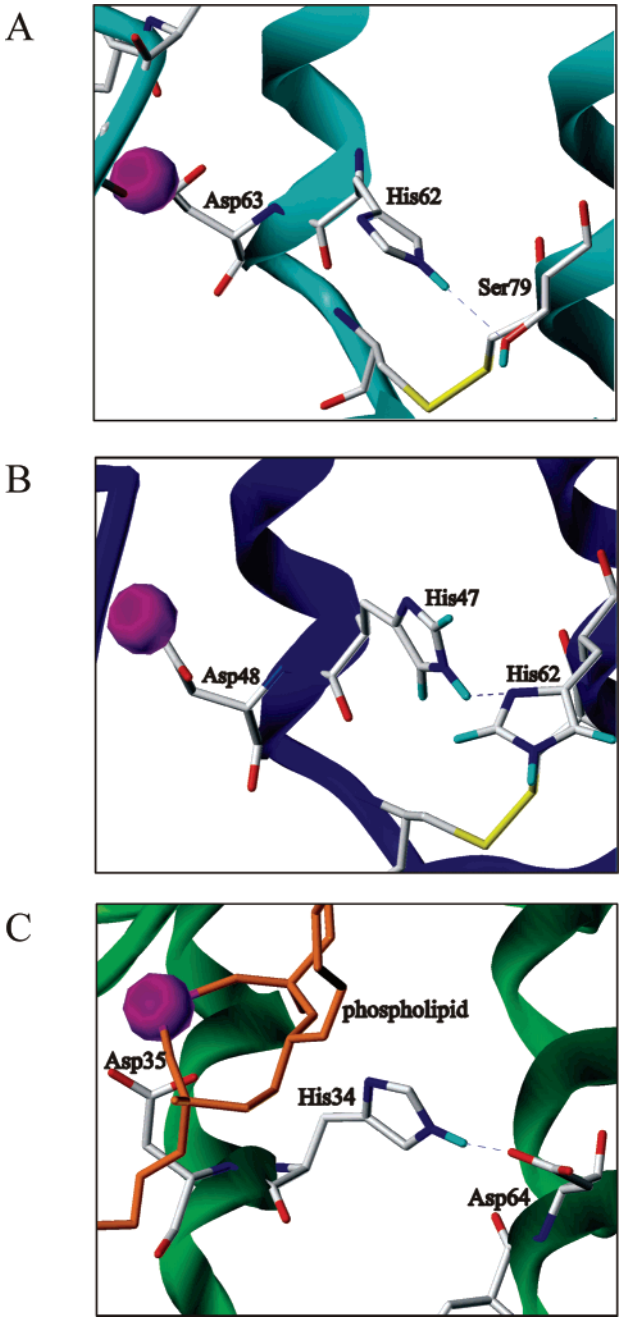

FIGURE 4: Details of the modeled active sites of AtsPLA$_2$-α (A) and AtsPLA$_2$-γ (B) in comparison to the active site crystal structure of bvPLA$_2$ (C).

from *D. caryophyllus*, *Po. tremulus*, *Go. arboreum*, *M. jalapa*, and three isoenzymes from *G. max*, whereas isoenzyme II from *Oryza sativa*, the enzyme from *L. esculentum*, and isoenzyme II from *N. tabacum* are characterized by an asparagine at this position. The enzymes from group XIA contain a histidine residue at this position. Figure 4 shows the geometry of the active sites of plant enzymes of groups XIB (AtsPLA$_2$-α) and XIA (AtsPLA$_2$-γ) in comparison to bvPLA$_2$. It shows that Ser79 (AtsPLA$_2$-α, Figure 4A) or His62 (AtsPLA$_2$-γ, Figure 4B) can adopt the role of the corresponding Asp residue in bvPLA$_2$ (Figure 4C) and bpPLA$_2$ and form a hydrogen bond with ϵN of the catalytic His62 (AtsPLA$_2$-α) or His47 residue (AtsPLA$_2$-γ).

It is well-known that a serine residue is the nucleophile in the hydrolysis of phospholipids by cPLA$_2$s and patatins as mentioned above. However, similarities with this type of PLA$_2$ can be excluded because Ser79 is not part of a consensus GXSXG(S) sequence which is a key feature of these enzymes. Furthermore, there is no similarity in the topology of the active sites of our model and that of patatin and cPLA$_2$ (*18*).

CONCLUSIONS

AtsPLA$_2$-α has been produced in a highly purified form for the first time. The biochemical characterization of this enzyme showed that the properties of the enzyme refolded from inclusion bodies were identical to those of the enzyme isolated in soluble form from the culture broth of *P. pastoris*.

Although AtsPLA$_2$-α and the well-known secretory animal PLA$_2$s possess low levels of overall identity in their primary structures, large parts of the tertiary structure of AtsPLA$_2$-α could be modeled on the basis of the known crystal structures of sPLA$_2$ from bovine pancreas and bee venom due to a high level of conservation of the primary structures in the calcium-binding loop and the active site. Consistent with this fact, the modeled tertiary structure of the active site region and the calcium-binding loop were shown to be very similar to the corresponding regions of the animal sPLA$_2$s, whereas the connecting structure elements show a great variability. A striking difference, however, was found in the amino acids that are essential for catalysis. The Asp residue of the catalytic His-Asp dyad in the animal enzymes is substituted with a Ser residue in AtsPLA$_2$-α and a His residue in AtsPLA$_2$-γ. The importance of the His62 and Ser79 residues as well as the Ca^{2+}-coordinating Asp63 residue of AtsPLA$_2$-α for activity was verified by amino acid exchanges by site-directed mutagenesis. The homology models show that Ser79 in AtsPLA$_2$-α and His62 in AtsPLA$_2$-γ could play a role in the catalytic mechanism similar to that of the corresponding Asp residues in animal sPLA$_2$s.

ACKNOWLEDGMENT

We thank Mrs. M. Sonntag for excellent technical assistance, K. Kölbel for supply of a sample of purified ppPLA$_2$, K. Kuppe and H. Hofmann for help in CD and fluorescence measurements, Dr. K.-P. Rücknagel (Max-Planck-Forschungsstelle für Enzymologie der Proteinfaltung, Halle, Germany) for N-terminal sequencing, and Mrs. Gersching for determination of the purity of the enzyme by mass spectroscopy. The donation of samples of phospholipids by Lipoid GmbH is gratefully acknowledged.

SUPPORTING INFORMATION AVAILABLE

Details of homology modeling and a figure showing a manual alignment of selected animal and plant sPLA$_2$s highlighting the regions considered for model construction and secondary structure elements (Figure 1) and a multiple-sequence alignment of the whole amino acid sequences for several sPLA$_2$s from plants (Figure 2). This material is available free of charge via the Internet at http://pubs.acs.org.

REFERENCES

1. Six, D. A., and Dennis, E. A. (2000) The expanding superfamily of phospholipase A$_2$ enzymes: Classification and characterization, *Biochim. Biophys. Acta 1488*, 1−19.
2. Balsinde, J., Winstead, V., and Dennis, E. A. (2002) Phospholipase A$_2$ regulation of arachidonic acid mobilization, *FEBS Lett. 531*, 2−6.
3. Berg, O. G., Gelb, M. H., Tsai, M.-D., and Jain, M. K. (2001) Interfacial enzymology: The secreted phospholipase A$_2$-paradigm, *Chem. Rev. 101*, 2613−2653.
4. Dessen, A., Tang, J., Schmidt, H., Stahl, M., Clark, J. D., Seehra, J., and Somers, W. S. (1999) Crystal structure of human cytosolic phospholipase A$_2$ reveals a novel topology and catalytic mechanism, *Cell 97*, 349−360.
5. Tanaka, H., Minakami, R., Kanaya, H., and Sumimoto, H. (2004) Catalytic residues of group VIB calcium-independent phospholipase A$_2$ (iPLA$_2$γ), *Biochem. Biophys. Res. Commun. 320*, 1284−1290.
6. Wang, X. (2001) Plant phospholipases, *Annu. Rev. Plant Physiol. Plant Mol. Biol. 52*, 211−231.
7. Stahl, U., Ek, B., and Stymne, S. (1998) Purification and characterization of a low-molecular-weight phospholipase A$_2$ from developing seeds of elm, *Plant Physiol. 117*, 197−205.
8. Stahl, U., Lee, M., Sjödahl, S., Archer, D., Cellini, F., Ek, B., Iannacone, R., MacKenzie, D., Semeraro, L., Tramontano, E., and Stymne, S. (1999) Plant low-molecular-weight phospholipase A$_2$s (PLA$_2$s) are structurally related to the animal secretory PLA$_2$s and are present as a family of isoforms in rice (*Oryza sativa*), *Plant Mol. Biol. 41*, 481−490.
9. Kim, J. Y., Chung, Y. S., Ok, S. H., Lee, S. G., Chung, W. I., Kim, I. Y., and Shin, J. S. (1999) Characterization of the full-length sequences of phospholipase A$_2$ induced during flower development, *Biochim. Biophys. Acta 1489*, 389−392.
10. Lee, H. Y., Bahn, S. C., Kang, Y.-M., Lee, K. H., Kim, H. J., Noh, E. K., Palta, J. P., Shin, J. S., and Ryu, S. B. (2003) Secretory low molecular weight phospholipase A$_2$ plays important roles in cell elongation and shoot gravitropism in *Arabidopsis*, *Plant Cell 15*, 1990−2002.
11. Bahn, S. C., Lee, H. Y., Kim, H. J., Ryu, S. B., and Shin, J. S. (2003) Characterization of *Arabidopsis* secretory phospholipase A$_2$-γ cDNA and its enzymatic properties, *FEBS Lett. 553*, 113−118.
12. Mansfeld, J., Dathe, K., Gebauer, S., and Ulbrich-Hofmann, R. (2004) Cloning, expression, and characterization of a plant secretory phospholipase A$_2$, *Chem. Phys. Lipids 130*, 48.
13. Lee, H. Y., Bahn, S. C., Shin, J. S., Hwang, I., Back, K., Doelling, J. H., and Ryu, S. B. (2005) Multiple forms of secretory phospholipase A$_2$ in plants, *Prog. Lipid Res. 44*, 52−67.
14. Ryu, S. B., Lee, H. Y., Doelling, J. H., and Palta, J. P. (2005) Characterization of a cDNA encoding *Arabidopsis* secretory phospholipase A$_2$-α, an enzyme that generates bioactive lysophospholipids and free fatty acids, *Biochim. Biophys. Acta 1736*, 144−151.
15. Rosahl, S., Schmidt, R., Schell, J., and Willmitzer, L. (1986) Isolation and characterization of a gene from *Solanum tuberosum* encoding patatin, the major storage protein of potato tubers, *Mol. Gen. Genet. 203*, 214−220.
16. Jung, K. M., and Kim, D. K. (2000) Purification and characterization of a membrane-associated 48-kilodalton phospholipase A$_2$ in leaves of broad bean, *Plant Physiol. 123*, 1057−1067.
17. Dhondt, S., Geoffroy, P., Stelmach, B. A., Legrand, M., and Heitz, T. (2000) Soluble phospholipase A$_2$ activity is induced before oxylipin accumulation in tobacco mosaic virus-infected tobacco leaves and is contributed by patatin-like enzymes, *Plant J. 23*, 431−440.

18. Rydel, T. J., Williams, J. M., Krieger, E., Moshiri, F., Stallings, W. C., Brown, S. M., Pershing, J. C., Purcell, J. P., and Alibhai, M. F. (2003) The crystal structure, mutagenesis, and activity studies reveal that patatin is a lipid acyl hydrolase with a Ser-Asp catalytic dyad, *Biochemistry 42*, 6696−6708.
19. Hirschberg, H. J., Simons, J.-W., Dekker, N., and Egmond, M. R. (2001) Cloning, expression, purification and characterization of patatin, a novel phospholipase A, *Eur. J. Biochem. 268*, 5037−5044.
20. Holk, A., Rietz, S., Zahn, M., Quader, H., and Scherer, G. F. E. (2002) Molecular identification of cytosolic, patatin-related phospholipases A from *Arabidopsis* with potential functions in plant signal transduction, *Plant Physiol. 130*, 90−101.
21. Hoffmann, G. E., Schmidt, D., Bastian, E., and Guder, W. G. (1986) Photometric determination of phospholipase A, *J. Clin. Chem. Clin. Biochem. 24*, 871−875.
22. Radvanyi, F., Jordan, L., Russo-Marie, F., and Bon, C. (1989) A sensitive continuous fluorometric assay for phospholipase A_2 using pyrene-labeled phospholipids in the presence of serum albumin, *Anal. Biochem. 177*, 103−109.
23. Segelke, B. W., Nguyen, D., Chee, R., Xuong, N. H., and Dennis, E. A. (1998) Structures of two novel crystal forms of *Naja naja naja* phospholipase A_2 lacking Ca^{2+} reveal trimeric packing, *J. Mol. Biol. 279*, 223−232.
24. Scott, D. L., Otwinowski, Z., Gelb, M. H., and Sigler, P. B. (1990) Crystal structure of bee-venom phospholipase A_2 in a complex with a transition-state analogue, *Science 250*, 1563−1566; (1991) *Science 252*, 764 (Erratum).
25. Dijkstra, B. W., Renetseder, R., Kalk, K. H., Hol, W. G., and Drenth, J. (1983) Structure of porcine pancreatic phospholipase A_2 at 2.6 Å resolution and comparison with bovine phospholipase A_2, *J. Mol. Biol. 168*, 163−179.
26. Dijkstra, B. W., Kalk, K. H., Hol, W. G., and Drenth, J. (1981) Structure of bovine pancreatic phospholipase A_2 at 1.7 Å resolution, *J. Mol. Biol. 147*, 97−123.
27. Bower, M. J., Cohen, F. E., and Dunbrack, R. L., Jr. (1997) Prediction of protein side-chain rotamers from a backbone-dependent rotamer library: A new homology modeling tool, *J. Mol. Biol. 267*, 1268−1282.
28. Laskowski, R. A., MacArthur, M. W., Moss, D. S., and Thornton, J. M. (1993) PROCHECK: A program to check the stereochemical quality of protein structures, *J. Appl. Crystallogr. 26*, 283−291.
29. Sippl, M. J. (1993) Recognition of errors in three-dimensional structures of proteins, *Proteins 17*, 355−362.
30. Verheij, H. M., Volwerk, J. J., Jensen, E. H. J. M., Pujik, W. C., Dijkstra, B. W., Drenth, J., and de Haas, G. H. (1980) Methylation of histidine-48 in pancreatic phospholipase A_2. Role of histidine and calcium ion in the catalytic mechanism, *Biochemistry 19*, 743−750.
31. Yu, B. Z., Rogers, J., Nicol, G. R., Theopold, K. H., Seshadri, K., Vishweshwara, S., and Jain, M. K. (1998) Catalytic significance of the specificity of divalent cations as KS* and kcat* cofactors for secreted phospholipase A_2, *Biochemistry 37*, 12576−12587.
32. Kumar, A., Sekharudu, C., Ramakrishnan, B., Dupureur, C. M., Zhu, G. H., Tsai, M.-D., and Sundaralingam, M. (1994) Structure and function of the catalytic site mutant Asp99 Asn of phospholipase A_2: Absence of the conserved structural water, *Protein Sci. 3*, 2082−2088.
33. Annand, R. H., Kontoyiannir, M., Penzotti, J. E., Dudler, T., Lybrand, T. P., and Gelb, M. H. (1996) Active site of bee venom phospholipase A_2: The role of histidine-34, aspartate-64 and tyrosine-87, *Biochemistry 35*, 4591−4601.
34. Edwards, S. H., Thompson, D., Baker, S. F., Wood, S. P., and Wilton, D. C. (2002) The crystal structure of the H48Q active site mutant of human group IIA secreted phospholipase A_2 at 1.5 Å resolution provides an insight into the catalytic mechanism, *Biochemistry 41*, 15468−15476.
35. Li, Y., and Tsai, M.-D. (1993) Phospholipase A_2 engineering. 10. The aspartate···histidine catalytic diad also plays an important structural role, *J. Am. Chem. Soc. 115*, 8523−8526.
36. Janssen, M. J., van de Weil, W. A., Beiboer, S. H., van Kampen, M. D., Verheij, H. M., Slotboom, A. J., and Egmond, M. R. (1999) Catalytic role of the active site histidine of porcine pancreatic phospholipase A_2 probed by the variants H48Q, H48N and H48K, *Protein Eng. 12*, 497−503.
37. Li, Y., Yu, B. Z., Zhu, B., Jain, M. K., and Tsai, M.-D. (1994) Phospholipase A_2 engineering. Structural and functional roles of the highly conserved active site residue aspartate-49, *Biochemistry 33*, 14714−14722.
38. Turini, P., Kurooka, S., Steer, M., Corbascio, A. N., and Singer, T. P. (1969) The action of phenylmethylsulfonyl fluoride on human acetylcholinesterase, chymotyrpsin and trypsin, *J. Pharmacol. Exp. Ther. 167*, 98−104.

BI052563Z